Statistical Process Monitoring of Between-Part and Within-Part Variations Using Independent Component Analysis

C. S. Cheng[1], H. P. Cheng[2], K. K. Huang[1]
[1]Department of Industrial Engineering and Management, Yuan-Ze University, Nei-Li, Taiwan, R.O.C.
[2]Department of Business Innovation and Development, Ming-Dao University, Peetow, Taiwan, R.O.C.
([1]ieccheng@saturn.yzu.edu.tw, [2]hpcheng@mdu.edu.tw)

Abstract - **The data collected from in-process measurement usually contain useful information about the nature of the source of process variability. In this paper, each variation source is assumed to generate a different spatial variation pattern in the quality characteristics measurements. The variation source might also reveal interesting temporal pattern over the data sample. The spatial variation pattern and temporal pattern caused by a variation source may turn out to be the observed within- and between-part variations in the monitoring of product measurements. The study reported in this paper aimed at applying independent component analysis (ICA) to monitor within- and between-part variations. Various monitoring statistics obtained from ICA are used to construct the control procedure. The average run length (ARL) is used to measure the abnormalities detection performance. An extensive comparison based on simulation study indicates that the ICA-based control charts perform better than conventional control charts in terms of ARL. The paper contributes to the monitoring of within- and between-part variations.**

Keywords – **within and between variations, ICA**

I. INTRODUCTION

In statistical process control (SPC), control charts are often used to discover the occurrence of assignable causes by monitoring the quality measurements collected over time on a process. Charting statistics outside the control limits reveal the occurrence of assignable causes of variation that must be searched or removed from the process. The estimate of chance causes variability used to establish the control limits of variable charts is often based on within-subgroup variability. In various practical applications, there are several independent variation sources that increase the entire variability of the measured data [1] and [2]. Every variation source may incur a different spatial variation pattern across the measured part characteristics. In addition, the variation source may also reveal temporal pattern over time. The information provided by variation pattern can facilitate the monitoring, diagnosis and eliminating of the root causes. As an example, consider a variation source follows a Bernoulli distribution. This type of variation sources is widely observed in manufacturing processes. The possible causes of these variation sources may be attributed to two parallel machines carrying out the identical operation or the usage of raw materials or components purchased from distinct suppliers.

The spatial variation pattern and temporal pattern caused by a variation source may turn out to be the observed within- and between-part variations in the monitoring of product measurements. An appropriate method for monitoring within- and between-part variations can provide a wealth of information and enable process operators to take proper actions when abnormalities are detected. It is useful to apply the so-called $I-MR-R/S$ chart [3] for monitoring this type of data. The combination of the three charts provides a method of assessing the stability of the between-part variation, and the within-part variation.

The aim of this research is to apply the independent component analysis (ICA) to address the monitoring of within- and between-part variations. We assume the spatial pattern caused by the within-part variation is a known nature of the current process and it is difficult or impossible to eliminate. In other words, this source of variability is treated as inherent. We concentrate on the monitoring the temporal pattern caused by variation sources.

II. INDEPENDENT COMPONENT ANALYSIS

Independent component analysis can be seen as a signal processing method used to transform observed multivariate data into statistically independent components that are expressed as linear combinations of observed variables. ICA is usually used for revealing latent factors that underlie sets of random variables, signals, or measurements. ICA was originally proposed to solve the blind source separation problem, which involves recovering independent source signals (e.g., different music, voice, or noise sources) after they have been linearly mixed by an unknown mixing matrix $\mathbf{A}$.

Several different algorithms for ICA have been proposed. In this section, we briefly describe the fast fixed-point ICA algorithm (FastICA) that was developed by Hyvärinen [4]. In the following discussions, scalars are written in italic lower case, vectors are written in bold lower case and matrices are written in bold capitals. In the ICA algorithm, we assume that d measured variables $x_1, x_2, \cdots, x_d$ are expressed as linear combinations of m ($\leq d$) unknown independent components $s_1, s_2, \cdots, s_m$. The measured variables and the independent components have means of zero (i.e., mean-centered). If we denote the random column vectors as $\mathbf{x} = [x_1, x_2, \cdots, x_d]^T$ and $\mathbf{s} = [s_1, s_2, \cdots, s_m]^T$, the relationship between them can be expressed as

$$\mathbf{x} = \mathbf{A}\mathbf{s} \quad (1)$$

978-1-4244-6481-4/10/$26.00 ©2010 IEEE

where $\mathbf{A}=[\mathbf{a}_1,\mathbf{a}_2,\cdots,\mathbf{a}_m] \in R^{d\times m}$ is the unknown mixing matrix. When n samples are available, the preceding relationship can be rewritten as

$$\mathbf{X}=\mathbf{AS}+\mathbf{E} \tag{2}$$

where $\mathbf{X}\in R^{d\times n}$ is the data matrix, $\mathbf{S}\in R^{m\times n}$ is the independent component matrix, and $\mathbf{E}\in R^{d\times n}$ is the residual matrix.

The basic problem of ICA includes the estimation of the mixing matrix $\mathbf{A}$ as well as the independent components $\mathbf{S}$ from the measurement data matrix $\mathbf{X}$. The purpose of ICA is equal to estimating a demixing matrix $\mathbf{W}$ so that the elements of the reconstructed vector $\hat{\mathbf{S}}$, written as:

$$\hat{\mathbf{S}}=\mathbf{WX} \tag{3}$$

get independently. The drawbacks of ICA include: (1) only non-Gaussian independent components can be reconstructed, (2) neither orders, powers, nor signs of independent components can be estimated. For mathematical convenience, we define that the independent components have unit variance. The first step in ICA is whitening or called sphering. Its purpose is to remove correlation between the observed variables. Measured variables $\mathbf{x}$ are transformed into uncorrelated variables $\mathbf{z}$ by using whitening. Consider a random vector $\mathbf{x}(k)$ at sample k, the whitening transformation can be expressed as

$$\mathbf{z}(k)=\mathbf{\Lambda}^{-1/2}\mathbf{U}^T\mathbf{x}(k)=\mathbf{Qx}(k) \tag{4}$$

where $\mathbf{Q}=\mathbf{\Lambda}^{-1/2}\mathbf{U}^T$ is called the whitening matrix, and $\mathbf{\Lambda}$ (diagonal matrix of its eigenvalues) and $\mathbf{U}$ (orthogonal matrix of eigenvectors) are created from the eigen-decomposition of the covariance matrix $E(\mathbf{xx}^T)=\mathbf{U\Lambda U}^T$. Following the transformation we have

$$\mathbf{z}(k)=\mathbf{Qx}(k)=\mathbf{QAs}(k)=\mathbf{Bs}(k) \tag{5}$$

where $\mathbf{B}=\mathbf{QA}$ is an orthogonal matrix as verified by the following relation:

$$E\{\mathbf{z}(k)\mathbf{z}^T(k)\}=\mathbf{B}E\{\mathbf{s}(k)\mathbf{s}^T(k)\}\mathbf{B}^T=\mathbf{BB}^T=\mathbf{I} \tag{6}$$

We can estimate $\mathbf{s}(k)$ from Eq. 6 as follows:

$$\hat{\mathbf{s}}(k)=\mathbf{B}^T\mathbf{z}(k)=\mathbf{B}^T\mathbf{Qx}(k) \tag{7}$$

From Eqs. (3) and (7), the relation between $\mathbf{W}$ and $\mathbf{B}$ can be rewritten as

$$\mathbf{W}=\mathbf{B}^T\mathbf{Q} \tag{8}$$

The objective of finding the matrix $\mathbf{B}$ is to make $\hat{\mathbf{s}}$ becomes as independent as possible. It has been shown that non-Gaussian represents independence. Non-Gaussianity is often measured by kurtosis and negentropy. The kurtosis method is simple but it is susceptible to the occurrence of outliers. The negentropy measure is built on the information theoretic quantity of entropy. Based on approximate form for the negentropy, Hyvärinen [4] presented a simple and highly efficient fixed-point algorithm for ICA, calculated over sphered zero-mean vectors $\mathbf{z}$. This algorithm computes one column of the matrix $\mathbf{B}$ and permits the identification of one independent component. The corresponding IC can be found using Eq. (7). We repeat the algorithm in order to calculate each independent component. After calculating $\mathbf{B}$, we can obtain $\hat{\mathbf{s}}(k)$ and demixing matrix $\mathbf{W}$ from Eqs. (7) and (8), respectively. For a detailed description of the FastICA algorithm, see Hyvärinen [4], and Hyvärinen and Oja [5].

III. MONITORING OF INDEPENDENT COMPONENTS

A.Monitoring of between-part and within-part variations

We use the following model to represent the between-part and within-part variations. Let $\mathbf{x}=[x_1,x_2,...,x_d]^T$ be a $d\times 1$ random vector that represents a set of d measured characteristics across a given part, and N represents the number of parts in the sample. We assume that $\mathbf{x}$ follows the model $\mathbf{x}=\mathbf{As}$. It is interpreted that there are m independent variation sources $\{s_i : i=1,2,\cdots,m\}$ that affect the measurement vector $\mathbf{x}$. The matrix $\mathbf{A}$ captures various variation sources result in within-part variations. Each source linearly affects x that is represented by the corresponding column of $\mathbf{A}$. The quantity $\mathbf{a}_i s_i$ defines the effect of the i^{th} source on $\mathbf{x}$. The variation pattern vector, $\mathbf{a}_i$, shows the spatial nature of the variation cause by the i^{th} source. Due to the reason that the elements of $\mathbf{s}$ are scaled to have unit variance, $\mathbf{a}_i$ also indicates the severity or magnitude of the i^{th} source. Throughout this paper, we assume that the noise variables associated with each elements of $\mathbf{x}$ are uncorrelated and have equal, but unknown variance. In other words, $\sigma_1^2=\sigma_2^2=\cdots=\sigma_d^2$. The random noise illustrates the accumulated effects of measurement noise and any natural variation not explained by the sources. In situations where the elements of $\mathbf{x}$ are similar entities gained through same measurement rules, this can be considered as a rational assumption. The purpose is to estimate each of the variation pattern vectors in $\mathbf{A}$, and the number of variation sources, m, using a sample of observations of $\mathbf{x}$. The estimated pattern vectors are used to clarify the characteristic of the spatial variation and furnish diagnostic knowledge about the root causes.

In the course of process diagnosis, it is usually helpful to estimate $\mathbf{A}$ as well as the source signals. The columns of $\mathbf{A}$ give information on the spatial nature of the variation patterns, on the other hand the estimated source signals give information in the temporal characteristic of the variation over the data sample. In the proposed approach, it is assumed that the fixed differences due to the measurement position are inherent to the process monitored. In other words, these variations are assumed to be very difficult or impossible to remove even after one makes a serious effort for improvement. The main focus of this paper is on monitoring the temporal variation of source signals.

B.On-line monitoring with ICA

This section describes the on-line monitoring using control statistics obtained from ICA. Some discussions about ICA monitoring with univariate SPC or multivariate SPC can be found in [6]-[9]. In the normal operating condition, designated $\mathbf{X}_{\text{normal}}$, $\mathbf{W}$ as well as $\hat{\mathbf{S}}_{\text{normal}}$ are obtained from the FastICA algorithm ($\hat{\mathbf{S}}_{\text{normal}} = \mathbf{W}\mathbf{X}_{\text{normal}}$) by assuming that the number of variables is equivalent to the number of independent components. The matrices $\mathbf{B}$, $\mathbf{Q}$, and $\mathbf{A}$ used in Eq. (5) are also obtained by whitening and the FastICA algorithm. As mentioned in the previous section, the data dimension can be decreased by choosing a small number of rows of $\mathbf{W}$ based on the assumption that the rows with the largest sum of squares coefficient hold the greatest effect on the variation of $\hat{\mathbf{S}}$. The a rows of $\mathbf{W}$ are chosen to constitute a reduced matrix $\mathbf{W}_{\text{d}}$ (dominant part of $\mathbf{W}$), and the remaining rows of $\mathbf{W}$ form a reduced matrix $\mathbf{W}_{\text{e}}$ (excluded part of $\mathbf{W}$). The reduced matrix $\mathbf{B}_{\text{d}}$ can be constructed by choosing the columns from $\mathbf{B}$ whose indices correspond to the indices of the rows selected from $\mathbf{W}$. The matrix $\mathbf{B}_{\text{d}}$ is computed directly using Eq. (8), i.e., $\mathbf{B}_{\text{d}} = (\mathbf{W}_{\text{d}}\mathbf{Q}^{-1})^T$. The matrix $\mathbf{B}_{\text{e}}$ is comprised by the remaining columns of $\mathbf{B}$. Then, new data for sample k, $\mathbf{x}(k)$, is transformed to new independent data vectors, $\hat{\mathbf{s}}_{\text{d}}(k)$ and $\hat{\mathbf{s}}_{\text{e}}(k)$, through the demixing matrices $\mathbf{W}_{\text{d}}$ and $\mathbf{W}_{\text{e}}$, i.e., $\hat{\mathbf{s}}_{\text{d}}(k) = \mathbf{W}_{\text{d}}\mathbf{x}(k)$ and $\hat{\mathbf{s}}_{\text{e}}(k) = \mathbf{W}_{\text{e}}\mathbf{x}(k)$, respectively. Lee *et al.* [7] introduced three control statistics for purposes of ICA process monitoring, namely I_{d}^2, I_{e}^2 and *SPE* (squared prediction error). When the I_{d}^2 statistic falls beyond the confidence interval, it shows that a process change has occurred in the model space. When the I_{e}^2 statistic falls beyond the confidence interval, it implies that a process change has taken place in the excluded model space. Finally, if the *SPE* statistic of residual space exceeds the limit, it implies the presence of process changes that break the ICA model. The control statistics at sample k can be defined as follows.

$$I_{\text{d}}^2(k) = \hat{\mathbf{s}}_{\text{d}}(k)^T \hat{\mathbf{s}}_{\text{d}}(k) \tag{9}$$

$$I_{\text{e}}^2(k) = \hat{\mathbf{s}}_{\text{e}}(k)^T \hat{\mathbf{s}}_{\text{e}}(k) \tag{10}$$

$$SPE(k) = \mathbf{e}(k)^T \mathbf{e}(k) \tag{11}$$

where $\hat{\mathbf{x}}(k)$ can be determined in the following manner:

$$\hat{\mathbf{x}} = \mathbf{Q}^{-1}\mathbf{B}_{\text{d}}\hat{\mathbf{s}}(k) = \mathbf{Q}^{-1}\mathbf{B}_{\text{d}}\mathbf{W}_{\text{d}}\mathbf{x}(k) \tag{12}$$

The control limits for the aforementioned control statistics must be calculated in order to utilize the ICA-based monitoring charts. To accomplish this purpose, we adopt the following procedures in the set-up phase of control charting procedure.

(1) Obtain time-series data when a process is operated under normal conditions. Normalize each row (variable) of the data matrix using the mean and standard deviation of each variable. That is, adjust it to a zero mean and unit variance, if necessary.

(2) Apply ICA to the normalized data, calculate a separating matrix $\mathbf{W}$, and determine independent components.

(3) Calculate I_{d}^2, I_{e}^2 and *SPE* values from normal operating data. The non-parametric kernel density estimator is applied to estimate the density function of the normal I_{d}^2, I_{e}^2 and *SPE* values. The point which occupies the $(1-\alpha)$% area of density function can be obtained and becomes the control limit of normal operating data (I_{d}^2, I_{e}^2 or *SPE* values), where α is the predetermined false alarm rate when the process is in normal operating mode.

IV. RESULTS

To illustrate the performance of the ICA-based SPC (ICA-SPC) over the conventional $I-MR-R/S$ chart, we apply these methods to the monitoring of diameters measured at nine locations on a part. In this comparison average run length (ARL) is used to assess the abnormality detection performance. The ARL is defined as the average number of points that must be plotted before an out-of-control condition is determined. Early detection of abnormalities is important for statistical process control, hence, a well-designed control method should give small ARL values when the process changes while maintaining a large ARL value when there is no change in the process.

Consider three uncorrelated source variables (signals) that have the following distributions:

$$s_1(k) = 2\cos(2.5k)\sin(0.1875k) \tag{13}$$

$$s_2(k) = \sin((\pi/4)*k) + \cos((\pi/8)*k) \tag{14}$$

$s_3(k) =$ uniformly distributed noises over the interval $[-\sqrt{3}, +\sqrt{3}]$ (15)

These sources $\mathbf{s} = [s_1, s_2, s_3]^T$ are linearly mixed as $\mathbf{x} = \mathbf{A}\mathbf{s}$ with the mixing matrix $\mathbf{A}_1$ defined in Eq. (16). Fig. 1 illustrates the spatial nature of the variation due to the above-mentioned sources. One data set obtained from the normal operating condition was used for analysis. We generated 1000 mixed data samples of $\mathbf{x}$ and add random noises with standard deviation 0.1 to the data. This data set was used to calculate a separating matrix for the ICA-based SPC and to estimate control limits. In this paper, the separating matrix was determined by the FastICA algorithm developed by Hyvärinen [4]. We set α to 0.0027 for each chart in the group of $I-MR-R$, which corresponds to the false alarm allowed in conventional control charting (i.e., 3-sigma control limits). The 99.73% confidence limits of each chart in $I-MR-R$ are obtained from kernel density estimation of normal operating condition data [8]. For a fair comparison, the confidence limits of $I_{\text{d}}^2 - I_{\text{e}}^2 - SPE$ are chosen to have in-control ARL that is as close as possible to that of $I-MR-R$ chart.

$$
A_1 = \begin{bmatrix} 0.8792 & 0.1815 & -0.7543 \\ 0.9217 & 0.2248 & 0.1233 \\ 0.9094 & -0.1513 & 0.8964 \\ -0.2412 & 0.4561 & -0.8128 \\ 0.1218 & -0.1183 & 0.3215 \\ 0.2619 & 0.5341 & 0.8972 \\ 0.4825 & 0.8481 & -0.8591 \\ -0.1315 & 0.9162 & 0.4583 \\ 0.5638 & 0.8685 & 0.7892 \end{bmatrix} \quad (16)
$$

The disturbance considered in this paper is a step change of s_1 by Δ units introduced at sample 33. Here, each ARL value is computed based on 10000 replicates. The detection results are summarized in Table I. The results reported for $I_d^2 - I_e^2 - SPE$ chart include different combinations of dominant ICs. The notation $IC_d = \{s_i, n_i\}$ represents the extracted dominant ICs include source signal and random noise. Studying the entries in Table I shows that the ARL value decreases as the shift size increases, regardless of the type of monitoring method. Examination of Table I shows that $I_d^2 - I_e^2 - SPE$ can detect abnormalities faster than $I - MR - R/S$ chart.

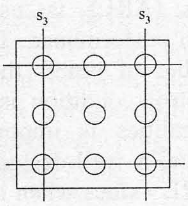

Fig. 1. The spatial nature of variation sources.

One of the monitoring results from using $I - MR - R$, and $I_d^2 - I_e^2 - SPE$ when the shift size is 2.0 is shown in Figs. 2 and 3, respectively. It is assumed that variation sources s_1, s_2, and s_3 are chosen as dominant ICs. The control limits denoted in dashed line are also exhibited in these figures. It is obvious that no indication of an out-of-control status is observed in the first 32 samples. As displayed in Figs. 2 and 3, the individuals chart detects the significant deviation at sample 43 (equivalent to a run length of 11) while I_d^2 chart detects it at sample 38. This example confirms that $I_d^2 - I_e^2 - SPE$ can detect abnormalities faster than $I - MR - R$ chart. One thing needs to be noted is that R chart may display a similar temporal pattern as that of I chart due to the fixed difference captured in A_1. This can be evident from comparing I and R charts in Fig. 2. The property implies that a specific assignable cause might result in out-of-control signal in two different charts and is complicated to deal with.

In the following the detection ability of the various monitoring statistics are compared. In the 10000 replicates, the number of abnormalities caught with each chart is termed as detection rate. The results, given in Tables II and III, indicate that the detection rate for each chart depends on the magnitude of the disturbance. However, from Table II it can be concluded that the detection rates for individuals chart are considerably higher than other charts as the shift size increases. Similar observation can be found for I_d^2 in the $I_d^2 - I_e^2 - SPE$ chart. It is also worthy to compare the detection abilities of various charts in the cases of structure change. It is assumed the source signals are mixed by matrix A_2 defined in Eq. 17. The results are summarized in Tables IV and V. As expected, the abnormalities are largely detected by R chart. For ICA-based SPC, the abnormalities are usually caught by I_e^2 and SPE charts.

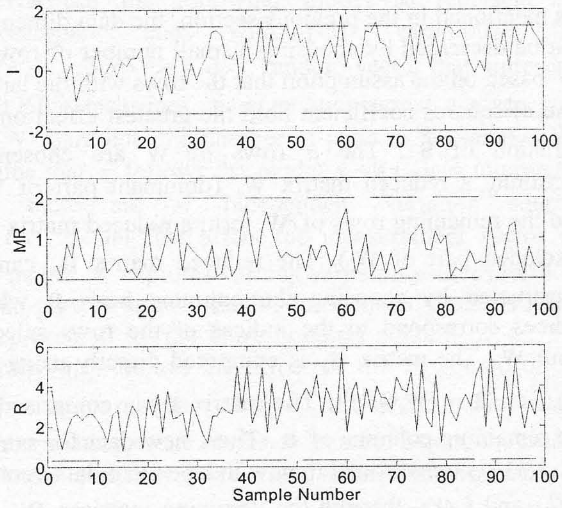

Fig. 2. $I - MR - R$ chart.

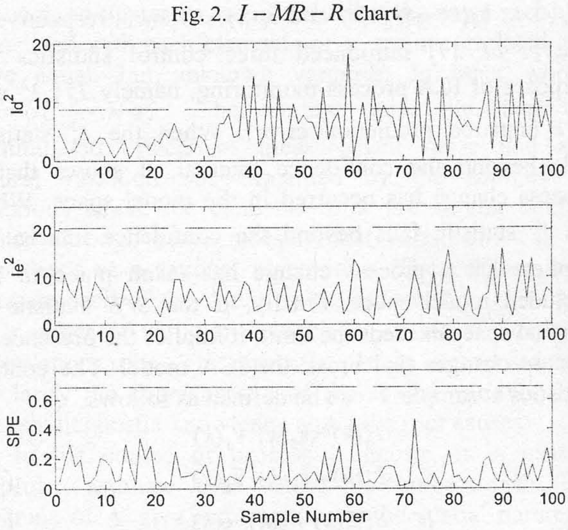

Fig. 3. $I_d^2 - I_e^2 - SPE$ chart.

$$
A_2 = \begin{bmatrix} 0.8792 & 0.1815 & -0.7543 \\ 0.9217 & 0.2248 & 0.1233 \\ 0.9094 & -0.1513 & 0.8964 \\ -0.2412 & 0.4561 & -0.8128 \\ 0.6209 & -0.1183 & 0.3215 \\ 0.5615 & 0.5341 & 0.8972 \\ 0.4825 & 0.1502 & -0.8591 \\ -0.1315 & 0.2159 & 0.4583 \\ 0.5638 & 0.1704 & 0.7892 \end{bmatrix} \quad (17)
$$

TABLE I ARL VALUES

Δ	$I - MR - R$	ICA	ICA	ICA	ICA	ICA

		$\mathrm{IC_d} = \{s_1, s_2, s_3\}$	$\mathrm{IC_d} = \{n_1, n_2, n_3\}$	$\mathrm{IC_d} = \{s_1, s_2\}$	$\mathrm{IC_d} = \{s_2, s_3\}$	$\mathrm{IC_d} = \{s_1\}$
0.0	169.4	170.5	172.0	171.6	171.1	171.7
0.1	173.3	170.2	167.1	164.7	68.58	57.11
0.2	166.6	155.5	154.0	129.0	28.52	26.67
1.0	49.93	12.55	34.96	6.213	6.703	6.537
2.0	5.323	4.442	5.355	3.044	2.965	2.966

TABLE II FAULT DETECTION RATES OF $I-MR-R$ CHART

Δ	I + others	MR + others	R + others	I only	MR only	R only	I and MR	MR and R	I and R	I, MR and R
0	3284	3433	3370	3200	3346	3367	84	3	0	0
0.1	3776	3396	2931	3685	3293	2919	91	12	0	0
0.2	4578	3191	2325	4496	3097	2313	82	12	0	0
1	4439	678	5158	4203	633	4891	8	39	230	2
2	6122	132	4108	5776	116	3746	0	16	346	0

TABLE III FAULT DETECTION RATES OF $I_d^2-I_e^2-SPE$ CHART

Δ	I_d^2 + others	I_e^2 + others	SPE + others	I_d^2 only	I_e^2 only	SPE only	I_d^2 and I_e^2	I_e^2 and SPE	I_d^2 and SPE	I_d^2, I_e^2 and SPE
0	2583	4128	3962	2573	3460	3295	6	663	5	1
0.1	2630	4106	3884	2621	3491	3268	4	611	5	0
0.2	3158	3730	3667	3144	3182	3120	8	541	7	1
1	9471	309	315	9422	236	254	34	46	22	7
2	9846	117	99	9799	76	67	30	15	21	4

TABLE IV FAULT DETECTION RATES OF $I-MR-R$ CHART FOR STRUCTURE CHANGE

	I +others	MR + others	R + others	I only	MR only	R only	I and MR	MR and R	I and R	I, MR and R
A_2	6	2595	9057	4	939	7399	0	1656	2	0

TABLE V

FAULT DETECTION RATES OF $I_d^2-I_e^2-SPE$ CHART FOR STRUCTURE CHANGE

	I_d^2 + others	I_e^2 + others	SPE+ others	I_d^2 only	I_e^2 only	SPE only	I_d^2 and I_e^2	I_e^2 and SPE	I_d^2 and SPE	I_d^2, I_e^2 and SPE
A_2	0	10000	8533	0	1467	0	0	8533	0	0

V. CONCLUSION

In this paper we have studied the monitoring of within- and between-part variations due to the spatial and temporal nature of the variation source. Monitoring statistics obtained from ICA are used to construct the control procedure. Simulation results showed the ICA-based control charts perform better than the conventional $I-MR-R/S$ in terms of ARL.

REFERENCES

[1] D. W. Apley, and H. Y. Lee, "Identifying spatial variation patterns in multivariate manufacturing processes: a blind separation approach," *Technometrics*, vol. 45, no. 3, pp. 220-234, 2003.

[2] K. S. Kim, and B. J. Yum, "Control charts for random and fixed components of variation in the case of fixed wafer locations and measurement positions," *IEEE Transactions on Semiconductor Manufacturing*, vol. 12, no. 2, pp. 214-228, 1999.

[3] Minitab, *Minitab 14.0 User's Guide*, State College, PA Minitab Inc., 2004.

[4] A. Hyvärinen, "Fast and robust fixed-point algorithms for independent component analysis," *IEEE Transactions on Neural Networks*, vol. 10, no. 3, pp. 626-634, 1999.

[5] A. Hyvärinen, and E. Oja, "Independent component analysis: algorithms and applications," *Neural Networks*, vol. 13, no. 4-5, pp. 411-430, 2000.

[6] M. Kano, S. Tanaka, S. Hasebe, I. Hashimoto, and H. Ohno, "Monitoring independent components for fault detection," *AIChE Journal,* vol. 49, no. 4, pp. 969-976, 2003.

[7] M. Kano, S. Hasebe, I. Hashimoto, and H. Ohno, "Evolution of multivariate statistical process control: application of independent component analysis and external analysis," *Computers and Chemical Engineering*, vol. 28, no. 6-7, pp. 1157-1166, 2004.

[8] J. M. Lee, C. K. Yoo, and I. B. Lee, "Statistical process monitoring with independent component analysis," *Journal of Process Control*, vol. 14, no. 5, pp. 467-485, 2004.

[9] J. M. Lee, S. J. Qin, and I. B. Lee, "Fault detection and diagnosis based on modified independent component analysis," *AIChE Journal*, vol. 52, no. 10, pp. 3501-3514, 2006.